J. Am. Soc. Mass Spectrom. (2011) 22:1645–1650
DOI: 10.1007/s13361-011-0173-1

RESEARCH ARTICLE

Diagnosing the Protonation Site of b_2 Peptide Fragment Ions using IRMPD in the X–H (X = O, N, and C) Stretching Region

Rajeev K. Sinha,[1] Undine Erlekam,[1] Benjamin J. Bythell,[2] Béla Paizs,[2] Philippe Maître[1]

[1]Laboratoire de Chimie Physique, Université Paris Sud, UMR8000 CNRS, Faculté des Sciences, Bât. 350, 91405 Orsay Cedex, France
[2]Computational Proteomics Group, German Cancer Research Center, Heidelberg, Germany

Abstract

Charge-directed fragmentation has been shown to be the prevalent dissociation step for protonated peptides under the low-energy activation (eV) regime. Thus, the determination of the ion structure and, in particular, the characterization of the protonation site(s) of peptides and their fragments is a key approach to substantiate and refine peptide fragmentation mechanisms. Here we report on the characterization of the protonation site of oxazolone b_2 ions formed in collision-induced dissociation (CID) of the doubly protonated tryptic model-peptide YIGSR. In support of earlier work, here we provide complementary IR spectra in the 2800–3800 cm^{-1} range acquired on a table-top laser system. Combining this tunable laser with a high power CO_2 laser to improve spectroscopic sensitivity, well resolved bands are observed, with an excellent correspondence to the IR absorption bands of the ring-protonated oxazolone isomer as predicted by quantum chemical calculations. In particular, it is shown that a band at 3445 cm^{-1}, corresponding to the asymmetric N–H stretch of the (nonprotonated) N-terminal NH_2 group, is a distinct vibrational signature of the ring-protonated oxazolone structure.

Key words: IRMPD, IR spectroscopy, Peptide fragmentation, Collision-induced dissociation, Oxazolone, Diketopiperazine

Introduction

Proton-driven amide bond cleavage is the key chemical reaction in mass spectrometry based peptide sequencing in proteomics [1–5]. The ionizing proton(s) play(s) a 2-fold role in the dissociation process by (1) weakening the amide bond acting as a catalyst and (2) attaching to dissociation product(s) allowing detection in the mass spectrometer. Hence, the characterization of the energetics and dynamics of protonation and "proton traffic" [6, 7] in the resulting ions are important issues for understanding the dissociation chemistry that leads to the b_n and y_n fragments formed upon collisional activation of (multiply-) protonated peptides. Peptides are multi-functional compounds with a plethora of likely protonation sites. Theoretical and experimental evidence exists for a mixture of initial protonation sites in some gas-phase peptides. Protonation can not only occur on the amino-terminus or basic side chains, but also on amide carbonyl oxygens. Theoretical study of protonated triglycine [8, 9] predicted that the two lowest energy structures correspond to carbonyl oxygen protonation. Additional experimental evidence [10, 11] for protonation of carbonyl oxygens has been recently provided by Wu and McMahon. Furthermore, direct evidence for the transfer of the ionizing proton has been provided by IR spectroscopy [12]. Some of the complexity of peptide fragmentation mass spectra is also due to the fact that upon collisional activation, b_n/y_n primary

While this paper was under review, a spectroscopic study of b_2 fragment of Protonated Triglycine in the NH and OH was published online [40].

Correspondence to: Philippe Maître; *e-mail:* philippe.maitre@u-psud.fr

Received: 3 April 2011
Revised: 17 May 2011
Accepted: 19 May 2011
Published online: 21 June 2011

fragment ions can subsequently dissociate by losing CO, NH_3, or H_2O, for example. Complex rearrangement chemistries can also occur upon peptide fragmentation and the formation of macrocyclic ring(s) has been proposed [13–17]. These studies indicate that the ionizing proton also plays an important role in rearrangement pathways of protonated peptides. In this context, the localization of the protonated sites of peptides and also of their fragments is an important issue.

Infrared spectroscopy has recently been critical for the structural characterization of peptide fragments. Most of the attention concerning peptide fragments has been devoted to b_n ions [12, 17–25]. Nonetheless, a_n CID fragments [26–28] as well as c_n fragment ions [29] generated via electron capture dissociation have also been investigated by IR spectroscopy. The highly intense and tunable IR beam delivered by free electron lasers (FELIX [30], CLIO [31]) is particularly well suited since it provides access to the so-called IR fingerprint region. As a result, structures bearing different functional groups can be clearly distinguished. It has been shown in particular that an IRMPD band appearing in the 1800–2000 cm^{-1} region is strongly diagnostic. Comparison with IR absorption determined using quantum chemical calculation shows that this band can be assigned to the oxazolone C = O stretching [22]. In the case of small b_n (n=2) ions, it was found that two strong IRMPD bands in the 1600–1800 cm^{-1} spectral range constitute IR signatures of diketopiperazine structures [18, 19, 24]. For larger b_n ($n \geq 4$) ions, formation of macrocyclic structures predicted by theory has been confirmed by IR spectroscopy [12, 17, 25]. Nonetheless, although it has been suggested that an IRMPD band appearing at ~1460 cm^{-1} could be an IR signature of a macrocycle [12], the spectral congestion in this IR region prevents clear conclusions. Alternatively, at higher photon energy, a broad band observed between 2500 and 2700 cm^{-1} could be the IR signature of a macrocycle structure [25].

In this paper, we report on IR spectroscopy of the b_2 fragment of doubly protonated YIGSR ions in the X–H (X = C, N, O) stretching region. Our main objective is to explore the potential of table-top laser systems for probing the structure of peptide fragments. A key question is whether the structural motifs characteristic of the different potential structures of peptide fragments have distinguishable IRMPD signatures. This work is a follow-up to a FEL IR spectroscopic investigation of the b_2 fragment of doubly protonated YIGSR in the 1000–2000 cm^{-1} spectral range. This IR fingerprint region is easily accessible with high fluence FELs, enabling a clear distinction between oxazolone and diketopiperazine isomers to be made [19, 24]. The absence of any signal corresponding to the characteristic absorption of the two CO stretches of the diketopiperazine isomers in the 1600–1800 cm^{-1} frequency window clearly showed that the b_2 fragment of doubly protonated YIGSR does not have a diketopiperazine structure [19]. Additionally, an unambiguous IR signature of an oxazolone can be found at higher photon energy for the b_2 ion of doubly protonated YIGSR; observed at 1920 cm^{-1} [19]. In the cases of protonated trialanine [18] and AGG [23], a band was observed at higher photon energies (1950 and 1970 cm^{-1}, respectively). Two types of oxazolone structures are possible depending on whether the proton is attached on the N-terminal amino group or on the oxazolone ring nitrogen (Scheme 1). Quantum chemical calculations show that the proton transfer from the former to the latter is associated with a red-shift of the absorption band of the oxazolone CO stretch. Nevertheless, the extent of the frequency-shift is system-dependent and can be relatively small. For example, the b_2 fragment of $[AGG + H]^+$ [23] provided a broad, asymmetric CO stretching band at 1970 cm^{-1}. It was concluded that a fraction of the N-terminally protonated oxazolone was responsible of the shoulder observed on the red-side of the CO stretching band. Conversely, the sharp bands observed at 1920 and 1950 cm^{-1} for the b_2 fragment of $[YIGSR + 2H]^{2+}$ [19] and $[AAA + H]^+$ [18], respectively, indicate that a single type of oxazolone structure is formed. The large variation in the frequency of the oxazolone CO stretching mode necessitates the use of calculated spectra for comparison to the two types of protonated oxazolone isomers in the IR fingerprint region. Without this, it is impossible to unambiguously conclude on the location(s) of the protona-

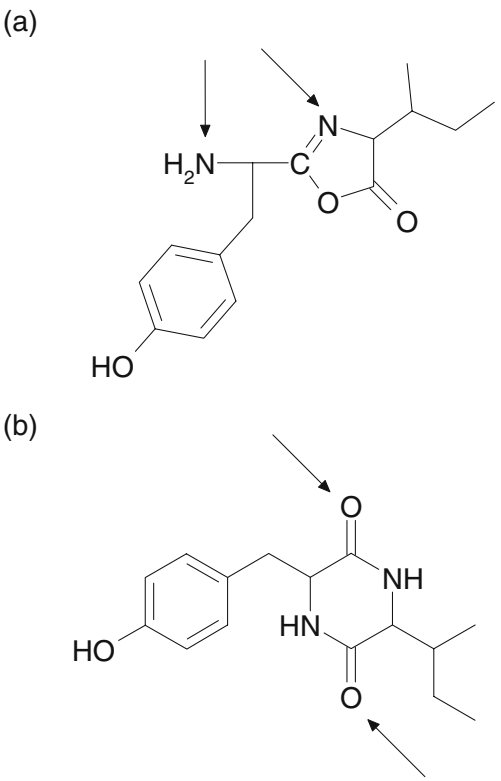

Scheme **1**. (a). Oxazolone structure for $YI_{oxazolone}$ with the N-terminal nitrogen and ring nitrogen protonation sites (respectively) indicated with arrows; (b) diketopiperazine structure for the YI sequence with the tyrosine oxygen (top) and isoleucine oxygen (bottom) protonation sites indicated with arrows

tion site of the oxazolone [18, 19, 23] of b_2 fragments. Conversely, the IR spectrum in the NH and OH stretching region as explored herein should provide more conclusive information regarding the localization of the proton on the peptide fragment.

Experimental

Materials

YIGSR [American Peptide Company (Sunnyvale, CA, USA)] was dissolved in $CH_3OH:H_2O=1:1$ with 2% acetic acid in a concentration range of 50–80 µmol.l^{-1} and was sprayed with conventional ESI conditions.

Mass Spectrometry and IRMPD Spectroscopy

IR spectra in the 2800–3800 cm^{-1} spectral range of the clusters ions were recorded using a 7 Tesla Fourier transform ion cyclotron resonance (FT-ICR) tandem mass spectrometer (Bruker Apex Qe) coupled with an optical parametric oscillator/amplifier (OPO/OPA from LaserVision) laser system [32, 33]. This laser system is pumped by an Innolas Spitlight 600 non-seeded Nd:YAG (1064 nm, 550 mJ/pulse, bandwidth ~1 cm^{-1}) laser running at 25 Hz and delivering pulses of 4–6 ns duration. Typical output energy of the OPO/OPA was 12–13 mJ/pulse at 3600 cm^{-1} with a 3–4 cm^{-1} (FWHM) bandwidth.

The ESI-formed doubly protonated YIGSR ions were mass selected and then allowed to collide with argon within the pressurized hexapole accumulation trap of the quadrupole-hexapole (Qh) interface of the 7 T hybrid FT-ICR mass spectrometer. Ions were then pulse-driven into the ICR cell, where b_2 ions were mass-selected and then subjected to IR irradiation. For strongly bound ions as in the present case, the output energy of the OPO/OPA system is not sufficient for efficiently inducing their fragmentation. With the OPO/OPA tuned on a vibrational transition of the mass-selected ion, a significant enhancement of the fragmentation signal can be observed by irradiating the ions using a few ms long CO_2 pulse [10 watt continuous wave (CW), BFi OPTiLAS, France] following each OPO/OPA pulse, the delay being on the order of ~1 µs. The total irradiation time was 1 s. This combination of a tunable OPO/OPA laser source with a broadband CO_2 laser has been successfully used recently for enhancing the sensitivity of IR spectroscopy of $[Mn(ClO_4)(H_2O)_{2-5}]^+$ and $[Mn_2(ClO_4)_3(H_2O)_{2-5}]^+$ cluster ions [34]. It should be noted that combination of tunable IR laser with line tunable CO_2 laser has been used previously [35, 36]. Finally an auxiliary CO_2 laser can also be useful for enhancing the spectroscopic sensitivity using the IR FEL at long wavelength, for probing metal-ligand modes for example [37].

Upon resonant vibrational excitation, dissociation of b_2 ions was monitored via the a_2 and a_1 peaks. The abundances of these photofragments and their corresponding b_2 precursors were recorded as a function of the IR wavelength in order to derive the IR action spectra where the IRMPD efficiency is plotted against the photon energy.

The spectral assignment of the infrared spectrum of b_2 YI fragment ions was done considering the same structures as those considered for the spectral assignment in the 1000–2000 cm^{-1} spectral range [19]. These structures were optimized at the B3LYP/6-31+G(d,p) level. The theoretical IR spectra were determined using harmonic frequencies scaled by a factor of 0.955. The calculated stick spectra were convoluted assuming a Gaussian profile with a 10 cm^{-1} full-width at half-maximum. The Gaussian set of programs [38] was used for all ab initio and DFT calculations.

Results and Discussion

The relative energies and free energies at room temperature of the four isomers considered for the spectral assignment are given in Table 1. The two lowest energy structures have a diketopiperazine motif (Scheme 1), and theory suggests that it is more favorable to protonate the tyrosine amide oxygen than that of the isoleucine. Structures with an oxazolone motif are predicted to be higher in energy. Theory predicts that the isomer corresponding to the protonation of the ring nitrogen is lower in energy than that with the proton attached to the N-terminal amino nitrogen. For the two oxazolone structures, it should be noted that charge solvation leads to a proton located between the ring and amino nitrogens.

The IR spectra of the b_2 fragment (YI sequence) are given in Figure 1. The experimental spectra (upper panel) are compared with the calculated absorption spectra associated with the lowest energy conformer of each of the four candidate structures. Three bands can be clearly observed experimentally (Figure 1a). An asymmetric band with a maximum at 3343 and a shoulder at 3360 cm^{-1} can be seen. Two sharp (FWHM ~ 15 cm^{-1}) spectral features are observed at 3445 and 3648 cm^{-1}. As discussed below, the range between 3300 and 3500 cm^{-1} is the most diagnostically useful part of the IRMPD spectrum. In order to improve the spectroscopic sensitivity in this spectral range, this part of the IR spectrum was recorded using an auxiliary CO_2 laser in conjunction with the tunable OPO/OPA laser whose power was specifically optimized in this spectral region.

Table 1. Relative energies (kJ/mol) of the four types of isomers described here

	Oxazolone Ring N prot.	Oxazolone Nter prot.	Diketopiperazine I oxygen prot.	Diketopiperazine Y oxygen prot.
H0 K	30.2	43.7	14.0	0.0
G298 K	28.5	40.6	12.8	0.0

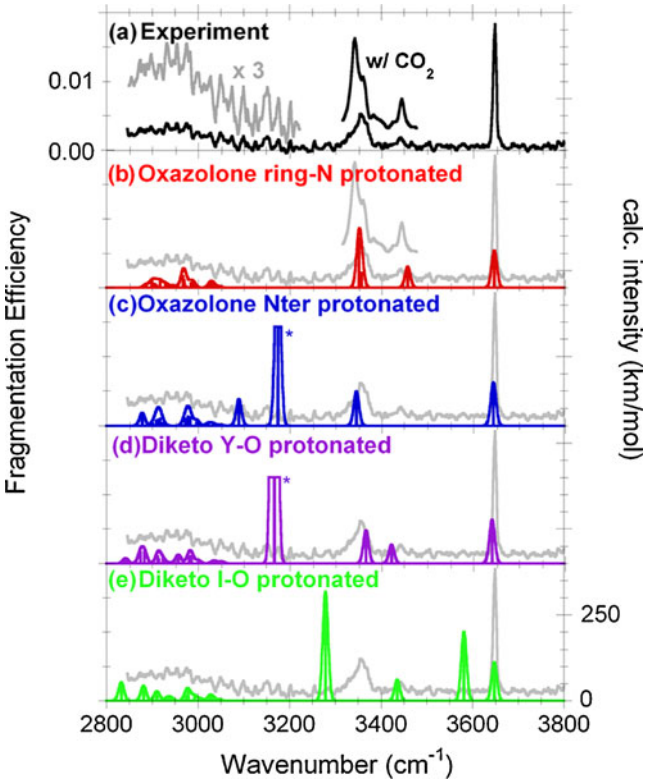

Figure 1. Experimental and calculated infrared spectra of the b_2 fragment of doubly protonated YIGSR in the spectral energy range between 2800 and 3800 cm^{-1}. **(a)** Experimental spectra recorded with the OPO/OPA laser in conjunction with an auxiliary CO_2 laser. Experimental conditions (see text) were optimized in order to improve the signal-to-noise ratio in the 3300–3500 cm^{-1} spectral range. **(b)-(e)** Calculated IR spectra of the four structures displayed in Scheme 1. In order to make the Figure clearer, the two bands (marked with an asterisk, at 3167 and 3175 cm^{-1} (see Table 1) in panels **(c)** and **(d)**, respectively) associated with large intensities (550 and 1703 $km.mol^{-1}$, respectively) were truncated. The calculated frequencies are scaled by 0.955, as are all of the frequency values in the text

Overall, the calculated IR absorption spectrum of the oxazolone type isomer protonated on the ring nitrogen (0.955 scaled) predicts the experimental spectrum qualitatively well (see Figure 1). In particular, the positions of the three sharp bands observed in the 3200–3500 cm^{-1} photon energy range nicely match those of the predicted IR active bands for the ring protonated oxazolone isomer. The calculated frequencies and associated intensities for the four isomers are given in Table 2 where they can be easily compared with the position of the experimental bands. As can be seen in this table, the band observed at 3648 cm^{-1} corresponds to the tyrosine OH stretching mode, which is predicted at about the same position for all isomers. The most useful part of the spectrum for the structural assignment is the region between 3300 and 3500 cm^{-1}. The IRMPD band observed at 3445 cm^{-1} can be assigned to the NH_2 asymmetric NH stretch calculated at 3458 cm^{-1} for the ring protonated oxazolone. Interestingly, the asymmetric shape of the IRMPD band with a maximum at 3343 cm^{-1} can also be interpreted considering the predicted IR spectrum of this isomer. As can be seen in Figure 1b, it has two nearly degenerate absorption bands: one at 3353 cm^{-1}, and another, less intense, at 3358 cm^{-1}, which could explain the observation of the shoulder observed at 3360 cm^{-1}. As shown in Table 2, the most intense absorption band predicted at 3353 cm^{-1} corresponds to the oxazolone N^+–H stretch, and the less intense absorption band at 3358 cm^{-1} corresponds to the NH_2 symmetric NH stretch.

Finally, it should be noted that a broad IRMPD band can be observed in the lower frequency part of the spectrum. This band is likely to correspond to the aliphatic and aromatic CH stretches which are predicted to be weakly IR active in the 2900–2990 and 3030–3070 cm^{-1} ranges, respectively. As observed in other cases with the same experimental setup [32], although the cross-section of each individual CH stretching mode is low, the near-degeneracy of these modes favors the multiple absorption process associated the IRMPD process. The width and the maximum (~2950 cm^{-1}) of the IRMPD band is consistent with the calculated frequencies of the alphatic and aromatic CH stretches, which are predicted to be in the 2900–2990 and 3030–3070 cm^{-1} spectral range, respectively.

Infrared spectroscopy allows for a clear determination of the protonation site of oxazolone. The predicted spectra of the two

Table 2. Experimental and theoretical (scaled by 0.955) frequencies in cm^{-1}, and calculated intensities (in parentheses) in km/mol

Experiment	Oxazolone ring N-protonated		Oxazolone N-terminally protonated		Diketopiperazine, Y-oxygen, protonated		Diketopiperazine, I-oxygen, protonated	
			NH_3^+ NH st	3090 (77)	HB OH^+-Phenyl	3167 (1703)		
			NH_3^+ NH st	3175 (550)				
							Y NH st	3279 (318)
3343	NH Oxa	3353 (144)	NH_3^+ NH st	3347 (99)				
3360	NH_2 s st	3358 (43)						
					I NH st	3368 (95)		
					Y NH st	3423 (54)		
							I NH st	3435 (61)
3445	NH_2 as st	3458 (61)						
							OH^+ st	3581 (201)
3648	Y OH	3648 (108)	Y OH	3645 (125)	Y OH	3643 (127)	Y OH	3648 (112)

HB = hydrogen-bonded; *s st* = symmetric stretch; *as st* = asymmetric stretch

oxazolone structures differing by the protonation site (Figure 1b and c) are very different. The oxazolone N-terminally protonated is characterized by three strongly red-shifted NH stretching modes predicted at 3090, 3175, and 3347 cm^{-1}. While an IRMPD band is observed at 3343 cm^{-1}, no IRMPD signal corresponding to the strongly IR active NH stretching mode predicted at 3175 cm^{-1} or to the one at 3090 cm^{-1} was observed. It could be argued that the output power of the OPO/OPA system is maximal at 3 μm but decreases when scanning towards the lower frequencies. Nevertheless, the fact that a broad IRMPD signal could be observed on resonance with the CH stretches suggests that the laser power is large enough for inducing the fragmentation of the oxazolone N-terminally protonated on resonance with the strongly IR active NH stretching mode predicted at 3175 cm^{-1}. It thus seems that the only oxazolone structure present under our experimental conditions corresponds to the proton attached to the ring nitrogen.

The IRMPD spectrum of the b_2 fragment of doubly protonated YIGSR ions in the IR fingerprint range reported by us [19] clearly showed that the diketopiperazine structures are not formed under similar experimental conditions. This was supported separately by transition structure calculations and gas-phase hydrogen/deuterium exchange experiments, which both arrived at this conclusion [39]. The calculated spectra of the diketopiperazine isomers either protonated on the oxygen of the Y or I residues are given in Figure 1d and e, respectively. These two spectra are significantly different from the experimental spectrum. In particular, they differ in the position of the O^+–H stretching mode. In the case of the I-oxygen protonated isomer, it is predicted at 3581 cm^{-1}, while it is significantly red-shifted to 3167 cm^{-1} in the case of the Y-protonated isomer. This strong shift to the red is characteristic of the hydrogen bond interaction of the OH^+ group with the aromatic ring of the Y side chain. Since no IRMPD band was observed near 3167 cm^{-1} or 3581 cm^{-1}, one can safely conclude that the diketopiperazine structures were not formed under our experimental conditions.

Conclusions

The IR spectrum of the b_2 ion of doubly protonated YIGSR peptide recorded in the 2800–3800 cm^{-1} region is strongly diagnostic for localizing the protonation site of this peptide fragment. Three main experimental bands centered at 3343 (with a shoulder at 3360 cm^{-1}), 3445, and 3648 cm^{-1} were observed. Overall, the agreement of the experimental IRMPD spectrum with the predicted IR absorption spectrum of the ring-protonated oxazolone isomer is remarkable. The band observed at 3445 cm^{-1}, corresponding to the asymmetric N–H stretch of the free N-terminal NH_2 group, is a clear vibrational signature of this isomer.

This structural assignment is fully consistent with that based on the IR spectrum recorded in the 1000–2000 cm^{-1} spectral range using the IR FEL. While the IR fingerprint region is well adapted for differentiating between isomeric forms, such as protonated-oxazolone and diketopiperazine of b_2 ions, the IR range provided by relatively low output power table top laser systems (2800–3800 cm^{-1}) is well suited to characterization of the protonation site. It should be stressed that a well resolved spectrum in the NH and OH stretching region could only be recorded by combining the table-top tunable laser with a high-power CO_2 laser. In contrast to the limited available access to IR FEL facilities worldwide, the present results combine two easily accessible lasers and provide a practical means of obtaining detailed structural information from products of tandem MS/MS experiments.

Acknowledgment

B.B. thanks the DKFZ for a guest scientist fellowship. B.P. is grateful to the Deutsche Forschungsgemeinschaft for a Heisenberg fellowship. Financial support by the European Commission EPITOPES project (NEST program, project no. 15367) is gratefully acknowledged. The authors are grateful to J. M. Ortega, J. P. Berthet, and E. Nicol for technical support.

References

1. Dongre, A.R., Jones, J.L., Somogyi, A., Wysocki, V.H.: Influence of peptide composition, gas-phase basicity, and chemical modification on fragmentation efficiency: evidence for the mobile proton model. *J Am Chem Soc* **118**(35), 8365–8374 (1996)
2. Paizs, B., Suhai, S.: Fragmentation pathways of protonated peptides. *Mass Spectrom Rev* **24**(4), 508–548 (2005)
3. Boyd, R., Somogyi, A.: The mobile proton hypothesis in fragmentation of protonated peptides: a perspective. *J Am Soc Mass Spectrom* **21**(8), 1275–1278 (2010)
4. Wysocki, V.H., Tsaprailis, G., Smith, L.L., Breci, L.A.: Special feature: commentary—mobile and localized protons: a framework for understanding peptide dissociation. *J Mass Spectrom* **35**(12), 1399–1406 (2000)
5. Bythell, B.J., Suhai, S., Somogyi, A., Paizs, B.: Proton-driven amide bond-cleavage pathways of gas-phase peptide ions lacking mobile protons. *J Am Chem Soc* **131**(39), 14057–14065 (2009)
6. Paizs, B., Csonka, I.P., Lendvay, G., Suhai, S.: Proton mobility in protonated glycylglycine and N-formylglycylglycinamide: a combined quantum chemical and RKKM study. *Rapid Commun Mass Spectrom* **15**(8), 637–650 (2001)
7. Csonka, I.P., Paizs, B., Lendvay, G., Suhai, S.: Proton mobility in protonated peptides: a joint molecular orbital and RRKM study. *Rapid Commun Mass Spectrom* **14**(6), 417–431 (2000)
8. Rodriquez, C.F., Cunje, A., Shoeib, T., Chu, I.K., Hopkinson, A.C., Siu, K.W.M.: Proton migration and tautomerism in protonated triglycine. *J Am Chem Soc* **123**(13), 3006–3012 (2001)
9. Paizs, B., Suhai, S.: Combined quantum chemical and RRKM modeling of the main fragmentation pathways of protonated GGG. *I. Cis-Trans Isomerization around Protonated Amide Bonds. Rapid Commun. Mass Spectrom.* **15**(23), 2307–2323 (2001)
10. Wu, R.H., McMahon, T.B.: Infrared multiple photon dissociation spectroscopy as structural confirmation for $GlyGlyGlyH^+$ and $AlaAlaAlaH^+$ in the gas phase. *Evidence for Amide Oxygen as the Protonation Site. J. Am. Chem. Soc.* **129**(37), 11312–11313 (2007)
11. Wu, R.H., McMahon, T.B.: Protonation sites and conformations of peptides of glycine ($Gly_{1–5}H^+$) by IRMPD Spectroscopy. *J Phys Chem B* **113**, 8767–8775 (2009)
12. Polfer, N.C., Oomens, J., Suhai, S., Paizs, B.: Infrared spectroscopy and theoretical studies on gas-phase protonated Leu-Enkephalin and its fragments: direct experimental evidence for the mobile proton. *J Am Chem Soc* **129**(18), 5887–5897 (2007)

13. Tang, X.J., Thibault, P., Boyd, R.K.: Fragmentation reactions of multiply-protonated peptides and implications for sequencing by tandem mass-spectrometry with low-energy collision-induced dissociation. *Anal Chem* **65**(20), 2824–2834 (1993)
14. Harrison, A.G., Young, A.B., Bleiholder, C., Suhai, S., Paizs, B.: Scrambling of sequence information in collision-induced dissociation of peptides. *J Am Chem Soc* **128**(32), 10364–10365 (2006)
15. Bleiholder, C., Osburn, S., Williams, T.D., Suhai, S., Van Stipdonk, M., Harrison, A.G., Paizs, B.: Sequence-scrambling fragmentation pathways of protonated peptides. *J Am Chem Soc* **130**(52), 17774–17789 (2008)
16. Harrison, A.G.: Peptide sequence scrambling through cyclization of b_5 ions. *J Am Soc Mass Spectrom* **19**(12), 1776–1780 (2008)
17. Erlekam, U., Bythell, B.J., Scuderi, D., Van Stipdonk, M., Paizs, B., Maitre, P.: Infrared spectroscopy of fragments of protonated peptides: direct evidence for macrocyclic structures of b_5 ions. *J Am Chem Soc* **131**(32), 11503–11508 (2009)
18. Oomens, J., Young, S., Molesworth, S., van Stipdonk, M.: Spectroscopic evidence for an oxazolone structure of the b_2 fragment ion from protonated tri-alanine. *J Am Soc Mass Spectrom* **20**(2), 334–339 (2009)
19. Bythell, B.J., Erlekam, U., Paizs, B., Maitre, P.: Infrared spectroscopy of fragments from doubly protonated tryptic peptides. *Chem Phys Chem* **10**(6), 883–885 (2009)
20. Chen, X.A., Steill, J.D., Oomens, J., Polfer, N.C.: Oxazolone versus macrocycle structures for Leu-Enkephalin b_2-b_4: insights from infrared multiple-photon dissociation spectroscopy and gas-phase hydrogen/deuterium exchange. *J Am Soc Mass Spectrom* **21**(8), 1313–1321 (2010)
21. Gucinski, A.C., Somogyi, A., Chamot-Rooke, J., Wysocki, V.H.: Separation and identification of structural isomers by quadrupole collision-induced dissociation-hydrogen/deuterium exchange-infrared multiphoton dissociation (QCID-HDX-IRMPD). *J Am Soc Mass Spectrom* **21**(8), 1329–1338 (2010)
22. Polfer, N.C., Oomens, J., Suhai, S., Paizs, B.: Spectroscopic and theoretical evidence for oxazolone ring formation in collision-induced dissociation of peptides. *J Am Chem Soc* **127**(49), 17154–17155 (2005)
23. Yoon, S.H., Chamot-Rooke, J., Perkins, B.R., Hilderbrand, A.E., Poutsma, J.C., Wysocki, V.H.: IRMPD spectroscopy shows that AGG forms an oxazolone b_2^+ ion. *J Am Chem Soc* **130**(52), 17644–17645 (2008)
24. Perkins, B.R., Chamot-Rooke, J., Yoon, S.H., Gucinski, A.C., Somogyi, A., Wysocki, V.H.: Evidence of diketopiperazine and oxazolone structures for HA b_2^+ Ion. *J Am Chem Soc* **131**(48), 17528–17529 (2009)
25. Chen, X., Yu, L., Steill, J.D., Oomens, J., Polfer, N.C.: Effect of peptide fragment size on the propensity of cyclization in collision-induced dissociation: oligoglycine b_2-b_8. *J Am Chem Soc* **131**(51), 18272–18282 (2009)
26. Bythell, B.J., Maitre, P., Paizs, B.: Cyclization and rearrangement reactions of a_n fragment ions of protonated peptides. *J Am Chem Soc* **132**(42), 14766–14779 (2010)
27. Oomens, J., Steill, J.D.: The structure of deprotonated tri-alanine and its a_3^- fragment anion by IR spectroscopy. *J Am Soc Mass Spectrom* **21**(5), 698–706 (2010)
28. Verkerk, U.H., Siu, C.K., Steill, J.D., El Aribi, H., Zhao, J.F., Rodriquez, C.F., Oomens, J., Hopkinson, A.C., Siu, K.W.M.: a_2 ion derived from triglycine: an N-1-protonated 4-imidazolidinone. *J Phys Chem Lett* **1**(5), 868–872 (2010)
29. Frison, G., van der Rest, G., Turecek, F., Besson, T., Lemaire, J., Maitre, P., Chamot-Rooke, J.: Structure of Electron-Capture Dissociation Fragments from Charge-Tagged Peptides Probed by Tunable Infrared Multiple Photon Dissociation. *J Am Chem Soc* **130**(45), 14916–14917 (2008)
30. Oepts, D., Van der Meer, A.F.G., Van Amersfoort, P.W.: The free-electron-laser user facility felix. *Infrared Phys Technol* **36**(1), 297–308 (1995)
31. Prazeres, R., Glotin, F., Insa, C., Jaroszynski, D.A., Ortega, J.M.: Two-colour operation of a free-electron laser and applications in the mid-infrared. *Eur Phys J D* **3**(1), 87–93 (1998)
32. Bakker, J.M., Besson, T., Lemaire, J., Scuderi, D., Maitre, P.: Gas-phase structure of a π-allyl-palladium complex: efficient infrared spectroscopy in a 7 T fourier transform mass spectrometer. *J Phys Chem A* **111**(51), 13415–13424 (2007)
33. Bakker, J.M., Sinha, R.K., Besson, T., Brugnara, M., Tosi, P., Salpin, J. Y., Maitre, P.: Tautomerism of uracil probed via infrared spectroscopy of singly hydrated protonated uracil. *J Phys Chem A* **112**(48), 12393–12400 (2008)
34. Sinha, R.K., Nicol, E., Steinmetz, V., Maitre, P.: Gas phase structure of micro-hydrated $[Mn(ClO_4)]^+$ and $[Mn_2(ClO_4)_3]^+$ ions probed by infrared spectroscopy. *J Am Soc Mass Spectrom* **21**(5), 758–772 (2010)
35. Peiris, D.M., Cheeseman, M.A., Ramanathan, R., Eyler, J.R.: Infrared multiple-photon dissociation spectra of gaseous ions. *J Phys Chem* **97** (30), 7839–7843 (1993)
36. Yeh, L.I., Okumura, M., Myers, J.D., Price, J.M., Lee, Y.T.: Vibrational spectroscopy of the hydrated hydronium cluster ions $H_3O^+(H_2O)_n$ (n= 1, 2, 3). *J Chem Phys* **91**(12), 7319–7330 (1989)
37. Lagutschenkov, A., Sinha, R.K., Maitre, P., Dopfer, O.: Structure and infrared spectrum of the Ag^+ phenol ionic complex. *J Phys Chem A* **114** (42), 11053–11059 (2010)
38. Frisch, M. J.; Trucks, G. W.; Schlegel, H. B.; Scuseria, G. E.; Robb, M. A.; Cheeseman, J. R.; Montgomery, J., J. A.;; Vreven, T.; Kudin, K. N.; Burant, J. C.; Millam, J. M.; Iyengar, S. S.; Tomasi, J.; Barone, V.; Mennucci, B.; Cossi, M.; Scalmani, G.; Rega, N.; Petersson, G. A.; Nakatsuji, H.; Hada, M.; Ehara, M.; Toyota, K.; Fukuda, R.; Hasegawa, J.; Ishida, M.; Nakajima, T.; Honda, Y.; Kitao, O.; Nakai, H.; Klene, M.; Li, X.; Knox, J. E.; Hratchian, H. P.; Cross, J. B.; Bakken, V.; Adamo, C.; Jaramillo, J.; Gomperts, R.; Stratmann, R. E.; Yazyev, O.; Austin, A. J.; Cammi, R.; Pomelli, C.; Ochterski, J. W.; Ayala, P. Y.; Morokuma, K.; Voth, G. A.; Salvador, P.; Dannenberg, J. J.; Zakrzewski, V. G.; Dapprich, S.; Daniels, A. D.; Strain, M. C.; Farkas, O.; Malick, D. K.; Rabuck, A. D.; Raghavachari, K.; Foresman, J. B.; Ortiz, J. V.; Cui, Q.; Baboul, A. G.; Clifford, S.; Cioslowski, J.; Stefanov, B. B.; Liu, G.; Liashenko, A.; Piskorz, P.; Komaromi, I.; Martin, R. L.; Fox, D. J.; Keith, T.; Al-Laham, M. A.; Peng, C. Y.; Nanayakkara, A.; Challacombe, M.; Gill, P. M. W.; Johnson, B.; Chen, W.; Wong, M. W.; Gonzalez, C.; Pople, J. A. *Gaussian Program Suite*; Gaussian, Inc.: Wallingford, CT, 2004.
39. Bythell, B.J., Somogyi, A., Paizs, B.: What is the structure of b_2 ions generated from doubly protonated tryptic peptides? *J Am Soc Mass Spectrom* **20**(4), 618–624 (2009)
40. Wang, D., Gulyuz, K., Stedwell, C. N., Polfer, N. C.: Diagnostic NH and OH Vibrations for Oxazolone and Diketopiperazine Structures: b_2 from Protonated Triglycine. *J Am Soc Mass Spectrom* (in press). doi:10.1007/s13361-011-0147-3